electronic state of the Pd atom is, however, 22 kcal/mol lower in energy than its d^9s^1 electronic state, and therefore it must form bonds with a bond energy of at least 22 kcal/mol to be stable. When two H_2O ligands are added to the Pd atom, this last electronic situation is induced.[32] In fact, the population analysis shows a tendency to depopulate the d orbitals, and it is speculated[32a] that with other ligands like CO or Ph_3, which are better electron acceptors, this depopulation should increase and therefore facilitate the oxidative addition of H_2 on a Pd atomic center with this more appropriate d^9s^1 electronic structure.

An analogous situation is found in our present results, that is, the tendency of the Cu atom to have a d^9s^2 electronic structure in order to be able to capture the H_2 molecule (see Table II). Naturally this electronic structure is facilitated by the presence of the electronic excited states of the Cu atom. We can notice as in the case of $Pd(H_2O)_2$ system that this electronic structure would be also induced by the presence of a ligand. In fact, if we consider in a speculative way the HCuH system as a metal complex model where H_2 addition can occur, then we do not need to resort to the photoexcitation of the Cu atom in order to give forth the pathway for the appropriate transformation of the electronic structure because now the HCuH complex has such structure. One more example of the correlation between the electronic excited states of a metal atomic center and the ligand effects toward its catalytic activity is found for NiH_2, CoH_2, and FeH_2.[32,33] In these cases the oxidative addition and the reductive elimination are feasible only when the excited states—^1D (d^9s^1), ^2F (d^8s^1), and ^3F (d^7s^2) of Ni, Co, and Fe, respectively—are considered, and the excited states is likewise the probable state for the conformations of L_nMH_2 complexes with M = Ni, Co, Fe.[32b,33]

To our knowledge, no previous studies have been carried out about the role played by the transition metal atom's excited states on a complete catalytic process. In fact, very few ab initio studies of a catalytic process itself, let alone the question of the excited states, have ever been attempted.[41-43] Also such studies were by necessity of relative modest computational sophistication, remaining at the SCF level. This is the case, for instance, of the studies[43] on titanium-aluminum catalytic complexes for Ziegler-Natta polymerization. From the theoretical results of ref 43 we now make some intriguing speculations about the possible participation of the excited states of the Ti atom. At least in ref 43 one thing was clearly established: that from the initiation of the reaction, (the entrance of the ethylene into the titanium coordination sphere), the aluminum atom, namely the cocatalyst, started to interact indirectly with the olefin. In that study the narrowing of the HOMO-LUMO gap and the constant changes in the s-d participation of the titanium on the highest occupied orbital throughout the process apparently hint at such participation of the Ti excited states. Therefore, a reexamination of the Ziegler-Natta process, perhaps at the pseudopotential level, in order to cut down the excessive size of the all-electron calculations,[43] but including configuration interaction, may be able to establish the role of the Ti excited states, and this appears to be quite attractive.

Acknowledgment. We express our gratitude to Dr. E. Poulain for all his worthy comments and effective help in some of the present calculations as well as his computational assistance, to our colleagues at the Laboratoire de Physique Quantique of Toulouse University for providing us with the CIPSI programs, and especially to Drs. Jean-Pierre Daudey and J. C. Barthelat. This research was partially supported by CONACYT, PVT/EN/NAL/81/1557.

Registry No. H_2, 1333-74-0; Cu, 7440-50-8.

(41) Dedieu, A. *Inorg. Chem.* **1980**, *19*, 375.
(42) Daudey, J. P.; Jeung, G.; Ruiz, M. E.; Novaro, O. *Mol. Phys.* **1982**, *46*, 67.
(43) Novaro, O.; Blaisten, E.; Clementi, E.; Giunchi, G.; Ruiz, M. E. *J. Chem. Phys.* **1978**, *68*, 2337.

Clay Modified Electrodes. 3. Electrochemical and Electron Spin Resonance Studies of Montmorillonite Layers

Deniz Ege, Pushpito K. Ghosh, James R. White, Jean-Francois Equey, and Allen J. Bard*

Contribution from the Department of Chemistry, The University of Texas at Austin, Austin, Texas 78712. *Received December 7, 1984*

Abstract: Films (about 30 nm to 3μm thick) of the clay mortmorillonite, with and without added poly(vinyl alcohol) (PVA), were cast on conductive substrates (SnO_2/glass, glassy carbon, platinum) and used as electrodes. Electron spin resonance of the incorporated probe, tempamine, and X-ray diffraction measurements showed that the films with clay alone were oriented, while those containing PVA were random and swollen. The electrochemistry of cationic species incorporated into the films, e.g., $Ru(bpy)_3^{2+}$, $Os(bpy)_3^{2+}$, $Fe(bpy)_3^{2+}$, is described; the effective diffusion coefficients of the Os and Fe species in these films were $\sim 10^{-12}$ cm^2 s^{-1}. Neutral (hydroquinone) and several anionic species, while not incorporated into the film, can diffuse through it to the substrate. Chronoamperometric and rotating disk electrode measurements were employed to study this diffusion. Catalytic hydrogen production at a clay/Pt/PVA film containing propyl viologen sulfonate was found.

The modification of electrode surfaces by coverage with a thin layer of a treated clay was recently reported from this laboratory.[1] Cationic species, e.g., $Ru(bpy)_3^{2+}$ (bpy = 2,2′-bipyridine), $Fe(bpy)_3^{2+}$, MV^{2+} (methyl viologen), could be incorporated into sodium montmorillonite films; for thicker films (ca. 3 μm) clay premixed with poly(vinyl alcohol) (PVA), with or without colloidal platinum, produced more durable films that more readily incorporated electroactive ions.[1] In a separate communication, clay films were shown to be potentially useful as supports for finely dispersed metals and metal oxides which can function as catalysts.[2] For example, ruthenium dioxide incorporated into the clay films promotes the oxidation of water in the presence of electrochemically produced $Ru^{III}(bpy)_2[bpy\text{-}(CO_2)_2]^+$ with regeneration of

(1) Ghosh, P. K.; Bard, A. J. *J. Am. Chem. Soc.* **1983**, *105*, 5691-5693.
(2) Ghosh, P. K.; Mau, A. W.-H.; Bard, A. J. *J. Electroanal. Chem.* **1984**, *169*, 315-317.

0002-7863/85/1507-5644$01.50/0

the Ru(II) complex. Clay films can also be used as supports for dispersed semiconductor particles. We have recently shown that illumination of free-standing clay/CdS films in the presence of propyl viologen sulfonate (PVS) and a sacrificial donor results in efficient formation of the blue viologen cation radical.[3] In this respect, the role of the clay films is similar to that for Nafion membranes containing CdS.[4]

Electrode surfaces modified with clay or other inorganic layers[5,6] offer advantages of high chemical stability, known and potentially controllable structural features, and, for large-scale applications, low cost. Recently intercalation properties of smectites have been studied by spectroscopic and photochemical methods.[7] The clay interlayers were shown to segregate $Ru(bpy)_3^{2+}$ efficiently from Na^+ and MV^{2+}, presumably because of differences in the sizes and solvation energies of these ions. Such special structural features, unique to these clays, have recently been exploited by Yamagishi et. al., who generated an enantiometric excess of $Co(bpy)_3^{3+}$ from a racemic mixture of $Co(bpy)_3^{2+}$, by electrochemical oxidation at such clay-modified electrodes.[8a] The electrochemical and photochemical investigation of thionine–clay electrodes was also reported recently.[8b]

In this paper, we describe further electrochemical studies of clay-modified electrodes and address the question of the structure of the clay film on the electrode surface using electron spin resonance (ESR) spectroscopy as a probe. Previous ESR work[9] had shown that films prepared from dilute clay suspensions (sodium hectorite, sodium montmorillonite) are oriented with the clay layers parallel to the substrate surface. We have also studied the diffusion of solution species through the clay films to determine whether electroactive ions in solution diffuse through a membrane-like film or whether the ions traverse the film through cracks and pinholes. Finally, we describe the electrochemical behavior of several redox couples such as $Ru(bpy)_3^{2+/3+}$, $Os(bpy)_3^{2+/3+}$, $Fe(bpy)_3^{2+/3+}$, and propyl viologen sulfonate (PVS) bound in clay films and discuss the role of PVA in the film structure. Well-behaved and durable clay films in the absence of PVA are shown to be useful, especially for thin films with extended soaking in electrolyte solution.[10]

Experimental Section

Materials. $Os(bpy)_3^{2+}$, $Fe(bpy)_3^{2+}$, potassium octacyanomolbydate(IV) dihydrate [$K_4Mo(CN)_8 \cdot 2H_2O$], and PVS were synthesized according to published procedures.[11-13] All other chemicals, 4-amino-2,2,6,6-tetramethylpiperidine (tempamine, Aldrich), $Ru(bpy)_3Cl_2 \cdot 6H_2O$ (Strem), hydroquinone (H_2O) (Strem), were reagent grade and used as received. Sodium montmorillonite (SWy-1), calcium montmorillonite (STx-1), and calcium hectorite (SHCa-1) were purchased from the Source Clay Minerals Repository (University of Missouri, Columbia, MO) and Fe-free montmorillonite was prepared according to the method of Mehra and Jackson.[14] All clays were used in Na^+-exchanged form. Slightly different methods of preparation of clay colloids were used, depending upon the exchangeable ion on the clay. Ten grams of SWy-1 were dispersed in 100 mL of distilled water under continuous stirring for 48 h. The dispersed SWy-1 was then centrifuged at 5000 rpm for 1 h and the precipitate, which contained a dark residue, was discarded. The supernatant solution was evaporated under vacuum at room temperature to incipient dryness and freeze dried. STx-1 (20 g/L) and SHCa-1 (10 g/L) were dispersed in 1 M NaCl for at least 48 h to exchange the Ca^{2+} ions with Na^+. These clays were then centrifuged (5000 rpm for 30 min) and washed with triply distilled H_2O to remove the excess Cl^-. Removal of excess Cl^- was continued by dialysis (tubing from Spectrapor, Spectrum Medical Industries, Inc.) until a negative test for Cl^- ions with 0.1 M $AgNO_3$ was obtained. The colloids were then evaporated almost to dryness and freeze dried. The colloids used for casting films were prepared by weighing the desired amount of freeze-dried clay and dispersing it in triply distilled water in an ultrasonic bath. Colloidal Pt was prepared from PVA (Type III, Sigma) and chloroplatinic acid by the method of Hirai et al.[15]

Apparatus. Instrumentation for electrochemistry was comprised of a PAR Model 173 potentiostat, a Model 175 universal programmer, and a Model 179 digital coulometer. Cyclic voltammograms were recorded on a Houston Instruments Model 2000 X–Y recorder; current–time transients were stored in a Norland 3001 digital oscilloscope. A Pine Instruments Model ASR-2 rotor was employed in rotating disk voltammetry measurements. All electrochemical experiments were carried out in an undivided three-electrode cell comprising a working electrode (transparent SnO_2, glassy carbon (GC) disk, or platinum disk), a sodium saturated or saturated calomel reference electrode (SSCE or SCE), and a platinum gauze counter electrode. Thickness measurements were made on dry films wth a Sloan Dektak surface profilometer. Absorption spectra were recorded on a Cary 17A spectrophotometer and ESR measurements were made with a Varian E-9 X-band spectrometer (100 kHz field modulation) equipped with a TE_{102} dual-sample cavity. X-ray diffraction (XRD) data were obtained with a General Electric (Model XRD-5) X-ray powder diffractometer with an Ortec (Model 401A) ratemeter. A Cu anode was operated at 35 kV and 15 mA.

Procedure. Films for electrochemical studies were cast on transparent SnO_2 plates, GC disks, or platinum disk electrodes. The procedure involved slow evaporation of a carefully measured volume (10–150 μL) of clay dispersions (2–14 g of clay/L). Films were prepared from colloidal clay alone, colloidal clay mixed with PVA (5 g/L), and colloidal clay mixed with a colloidal Pt/PVA solution (0.24 g/L of Pt; 4 g/L of PVA) in 1:1 (v/v) $EtOH/H_2O$. Thinner films were obtained from dilute clay dispersions. Very thin (0.03–0.2 μm) clay films were spin coated on a GC or SnO_2 electrode with use of a solution containing colloidal clay and EtOH. The substrate (GC or SnO_2) was spun at 8000 rpm and was heated with a heat gun for 15 s first, before applying the clay solution. The thickness of these films was controlled by the number of drops of solution applied. Clay films were usually air-dried overnight (12 h). To speed up the evaporation of the solvent, the SnO_2 slides were placed above a hot plate (not in direct contact) or oven to yield film temperatures of 34 °C. The way the clay electrodes were dried strongly affected the electrochemical response at such electrodes (i.e., the drier the films were, the longer they had to be soaked to obtain any signal). Film samples for ESR measurements were cast on polyethylene slides or SnO_2-coated glass and were prepared either from pure clay suspensions or from clay suspensions containing PVA.

Ions were incorporated into the film matrix by soaking the electrodes in aqueous solutions of these ions. For studies with $Ru(bpy)_3^{2+}$, the concentration of the metal complex within the clay films was varied by immersing the electrode for different lengths of time in a 1 mM $Ru(bpy)_3^{2+}$ solution. The $Ru(bpy)_3^{2+}$ concentration was determined from absorbance measurements for films cast on transparent SnO_2 electrodes. For the ESR measurements tempamine was mixed with the colloidal clay before casting the film. The tempamine concentration corresponded to 2–5% of the cation exchange capacity (cec) of the clay used.

Results and Discussion

Sodium montmorillonite and sodium hectorite possess a sheet-like structure, each sheet consisting of two inverted tetrahedral layers sharing their apical oxygen with an octahedral layer.[16] While the tetrahedral layers are generally silicate sheets, different ions can be found in the octahedral layer. For example, the electroneutral mineral pyrophyllite has two out of three octahedral sites occupied by Al(III), while in talc, all three octahedral sites are occupied by Mg(II). Substitution of 15% of Al(III) by Mg(II) and ~8% of the Mg(II) by Li(I) results in the commonly observable structures of montmorillonite and hectorite, respectively. The cation exchange capacity originates from a lack of electro-

(3) Ghosh, P. K.; White, J. R.; Enea, O.; Bard, A. J., unpublished results.
(4) Krishnan, M.; White, J. R.; Fox, M. A.; Bard, A. J. *J. Am. Chem. Soc.* **1983**, *105*, 7002.
(5) Zak, J.; Kuwana, T. *J. Am. Chem. Soc.* **1982**, *104*, 5514; *J. Electroanal. Chem.* **1983**, *150*, 645.
(6) Murray, C. G.; Nowak, R. J.; Rolison, D. R. *J. Electroanal. Chem.* **1984**, *164*, 205.
(7) Ghosh, P. K.; Bard, A. J. *J. Phys. Chem.*, in press.
(8) (a) Yamagishi, A.; Aramata, A. *J. Chem. Soc., Chem. Commun.* **1984**, 119–120. (b) Kamat, P. *J. Electroanal. Chem.* **1984**, *163*, 389.
(9) McBride, M. B. *Clays Clay Miner.* **1979**, *27*, 97.
(10) A preliminary note with similar findings appeared after submission of this paper: Liu, H.; Anson, F. C. *J. Electroanal. Chem.* **1985**, *184*, 411–417.
(11) Gaudiello, J. G.; Bradley, P. G.; Norton, K. A.; Woodruff, W. H. Bard, A. J. *Inorg. Chem.* **1984**, *23*, 3.
(12) Furman, N. H.; Miller, C. O. *Inorg. Synth.* **1950**, *3*, 160.
(13) Maverick, A. W.; Najdzionek, J. C.; Mackenzie, O.; Nocera, D. G.; Gray, H. B. *J. Am. Chem. Soc.* **1983**, 105 1878.
(14) Mehra, O. P.; Jackson, M. L. "Clays and Clay Minerals: Proceedings of the Seventh National Conference", Swineford, A., Ed.; 1958; also, see ref 20a in ref 7.
(15) Hirai, H.; Nakau, Y.; Toshima, H. *J. Macromol. Sci., Chem.* **1979**, *A13*, 727.
(16) Theng, B. K. G. "Formation and Properties of Clay–Polymer Complexes", Developments in Soil Science 9; Elsevier: Amsterdam, 1979.

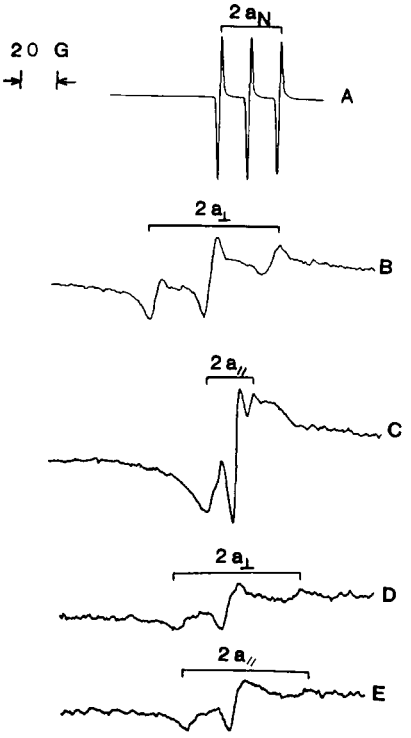

Figure 1. ESR spectra of tempamine incorporated into sodium montmorillonite films (2% cec): (A) aqueous 9.0×10^{-4} M tempamine, no clay; (B) cast sodium montmorillonite film oriented perpendicular to field; (C) same as B, but oriented parallel to field; (D) cast sodium montmorillonite/PVA/Pt film oriented perpendicular to field; (E) same as D but oriented parallel to field.

neutrality in these clays. The phyllosilicate sheets are stacked in the solid state (presumably due to van der Waals interactions), but because the layer lattice structure is expandable, ions and molecules can penetrate between the sheets, resulting in increased basal spacings and, in some cases, complete cleavage of the sheets. The clay particles, in fact, tend to break apart into isolated platelets when suspended in water.[17] It is of interest, in connection with our studies on modified electrodes, to understand the restructuring process when dilute suspensions of these clays are air dried to form thin films on electrode surfaces. In particular we wish to note any differences in film structure orientation which may result from the treatment of the clay dispersions with colloidal Pt/PVA or PVA.

Film Orientation. ESR of Tempamine(1+) (1) in Dry Clay Films. Tempamine(1+) (**1**) has been shown to be a useful probe for the elucidation of the structure of hectorite films.[9] In general,

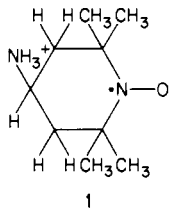

1

nitroxide spin probes have a single unpaired electron which resides mainly in the nitrogen $2p\pi$ orbital (i.e., perpendicular to the –N–O moiety). Dilute aqueous solutions of **1** produce a three-line ESR spectrum due to couplng of the eletronic spin with the nitrogen nucleus ($I = 1$) (Figure 1A). The hyperfine coupling constant, a_N, is 16.8 G. Tempamine incorporated into the hectorite films as described in the Experimental Section and subsequently air dried resulted in a coherently oriented assembly of probes such that the g and a_N values characterizing the resulting anisotropic ESR spectrum depended upon whether the film was oriented parallel or perpendicular to the magnetic field.[9] We observed similar behavior upon incorporating **1** (2% cec) into sodium montmorillonite (SWy-1) films which were subsequently air dried. The anisotropic ESR spectrum showed hyperfine coupling constants $a_\perp = 33.5$ G and $a_\parallel = 11.8$ G for films oriented perpendicular and parallel to the magnetic field, respectively (Figure 1B,C). The difference $a_\perp - a_\parallel$ is 21.7 G which is similar to the difference for a highly ordered assembly of probes.[9] In agreement with previous work, these results indicated that the clay platelets form films in which the phyllosilicate sheets are all parallel to the substrate surface. The incorporated tempamine probe is motionally restricted within the dried film with the nitrogen $2p\pi$ orbital perpendicular to the clay laminae. Thus, the maximum and minimum values of a_N are observed when the field is oriented perpendicular and parallel to the phyllosilicate sheets, respectively. The orientation of the sodium montmorillonite film is shown schematically in Figure 2A.

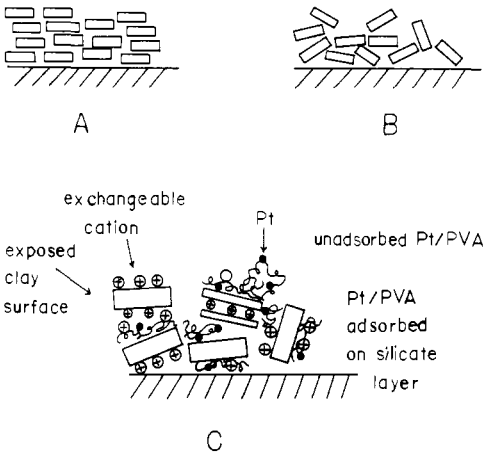

Figure 2. Proposed orientation of the clay films: (A) clay, (B) clay–Pt/PVA, (C) schematic of the proposed microstructure for clay–Pt/PVA.

Table I. X-ray Diffraction Results

film conditions[a]	2θ (deg)	basal spacing (Å)	fwhm[c] (deg)
S Tx-1[b] (air dried 12 h)	6.5	13.6	1.2
S Tx-1 (soaked 0.5 h in H_2O)	6.1	14.7	1.1
S Tx-1/0.1% PVA (1:1) (air dried 12 h)	4.3	20.5	1.1
S Tx-1/0.1% PVA (1:1) (soaked 0.5 h in H_2O)		>80	

[a] Films cast on SnO_2 glass and contain 2% cec tempamine. [b] S Tx-1 obtained in Ca^{2+} form and ion exchanged to Na^+ form. [c] Fwhm = full width at half maximum peak height.

Films cast with sodium montmorillonite/PVA containing tempamine prepared in the same way as films not containing PVA showed the same ESR spectra, independent of their orientation in the magnetic field (Figure 1D,E). The value of $a_\perp$ was 31.8 G, similar to the value for montmorillonite alone, and $a_\parallel$ was not resolvable. This behavior is indicative of probes that are motionally restricted and ordered on a microscope scale, but the indifference to orientation in the magnetic field implies a chaotic collection of microregions.[19] The proposed orientation of sodium montmorillonite/Pt/PVA films is shown schematically in Figure 2B.

X-ray Diffraction of Clay Layers. In addition to the ESR measurements, we also made X-ray diffraction measurements on the same films. X-ray diffraction patterns for clay films exhibit a prominent peak in the region of $2\theta < 10°$. This (001) reflection

(17) Van Olphen, H. "An Introduction to Clay Colloid Chemistry"; Wiley: New York, 1977.
(18) "Crystal Structure of Clay Minerals and their X-ray Identification"; Brindley, G. W., Brown, G., Eds.; Minerological Society: London, 1980; p 170.
(19) Berliner, L. J., Ed. "Spin Labeling, Theory and Applications"; Academic Press: New York, 1976; p 388.

corresponds to the basal spacing, the distance between repeating 2:1 units including intercalated ions and solvent.[18] The values, for various film conditions, are tabulated in Table I. These results demonstrate that casting films with PVA results in an increased basal spacing, suggesting that PVA is adsorbed on the exchange surface of the clay. Since the peak widths are similar, one can assume a uniform distribution of PVA on the clay surface; a nonuniform distribution would result in broad asymmetric peaks.[18] When the above films are hydrated by soaking in distilled water for 0.5 h, the film without PVA showed an increase in the basal spacing of 1.1 Å, due to solvent uptake. No time-dependent study was performed to see if larger basal spacings could be measured for prolonged soaking periods. Similarly, film cast with PVA show no peak in the region of $2\theta < 10°$. This suggests that basal spacings are >80 Å. Under these conditions, there is probably little face-to-face association of individual platelets in the randomly oriented film.

Structure of Clay Films. The above results clearly distinguish differences in film orientation for films cast in the absence and presence of PVA. However, what are the microstructures of these films? Pure clay films are simply a face-to-face aggregate of stacks of individual clay sheets. The structure of such clay sheets is well-known from previous work.[17] On the other hand, the answer is less clear for films cast from clay/PVA mixtures, since strong interactions between clay and PVA lead to a modification of the clay structure and, presumably, of the film structure as well. Greenland[20] has shown that PVA is strongly adsorbed on clays (by an entropy driven process) and that at maximum adsorption [0.8 g PVA (12% residual acetyl groups)/g of clay] the polymer coating was sufficient to form a layer 10 Å deep on the internal and external surfaces of sodium montmorillonite. Adsorption is evident from the gel-like appearance of the mixture, and the degree of adsorption is dependent upon the nature of the exchangeable cation, the concentration of clay suspension, the type of PVA used, and the method of mixing.[20] Although the presence of colloidal Pt in the mixture is a complicating factor, we presume that adsorption of Pt/PVA on the clay surface occurs by an analogous process in our system as well. The clay–Pt/PVA mixture turns gelatinous also as reported earlier for the clay–PVA system; we have not established the degree of adsorption. If all of the Pt/PVA is adsorbed, 35–40% of the clay surface would be coated with the polymer in our mixtures (4 g/L of PVA; 12 g/L of clay). On the basis of the XRD results, we do not believe that two different phases, one with PVA and PVA-free, exist. Interlamellar penetration by the polymer increases the basal spacing between clay layers. Such a situation, therefore, reduces the tendency toward face-to-face aggregtion (as is found in pure clay films) resulting in a more random orientation of the clay sheets. This is evident from the ESR and XRD experiments. Cyclic voltammetric experiments also indicate that the presence of PVA changes the nature of the films, thus facilitating the rate of electron transfer. The proposed microstructure of the clay/Pt/PVA films is shown schematically in Figure 2C.

Diffusion of Solution Species through Clay Films. Cations, such as $Ru(bpy)_3^{2+}$, are exchanged into the clay film and held with sufficient strength so that they are not quickly leached out when the filmed electrode is transferred into a solution containing only supporting electrolyte. Studies of such strongly absorbed species are described in the following sections. Neutral (H_2Q) or anionic species ($C_2O_4^{2-}$, $Mo(CN)_8^{4-}$, I^-) are not strongly absorbed, and electrochemical investigation of these can provide information about the presence of pinholes or channels in the film or the behavior of the films as membranes. These investigations parallel those made with polymer layers on electrode surfaces[21-23] by chronoamperometric or rotating disk electrode techniques. In chronoamperometric studies the current–time (i–t) curve at the filmed electrode is compared to that at the bare electrode (i_d–t),

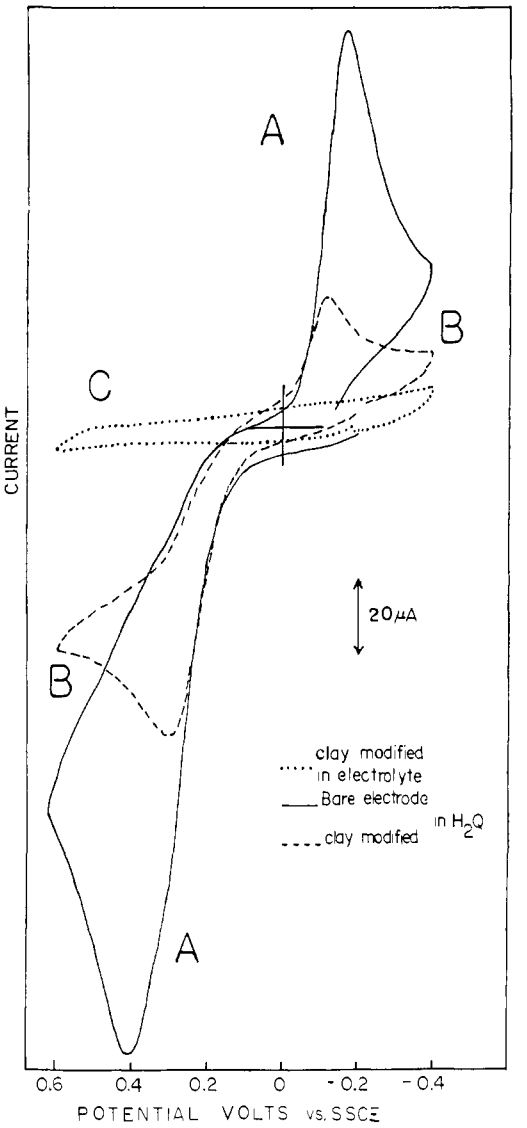

Figure 3. Cyclic voltammograms at a clay-modified electrode at a sweep rate of 100 mV s^{-1}: (A) at a bare electrode in 1 mM H_2Q; (B) in 1 mM H_2Q; (B) in 1 mM H_2Q, pH 7 phosphate buffer; (C) in pH 7 phosphate buffer.

and the differences fit to a pinhole[24,25] or membrane[21] model. In rotating disk electrode investigations, the limiting disk current (i_l) is measured as a function of angular velocity (ω).[26-28]

Consider the oxidation of hydroquinone (H_2Q) at a clay-modified electrode when a glassy carbon electrode modified with a montmorillonite film (STx-1-PVA-Pt) is dipped in a solution containing 1 mM hydroquinone (H_2Q): a cyclic voltammogram is obtained which has the same shape as a voltammogram recorded at a bare electrode but with lower peak currents (compare parts A and B of Figure 3). When the electrode is removed from this solution and placed in pure supporting electrolyte (pH 7 phosphate buffer) and a voltammogram taken immediately, the H_2Q waves have disappeared (Figure 3C), indicating rapid loss of H_2Q from the film. Penetration of H_2Q through the clay film was investigated by chronoamperometry of the bare and filmed electrode in a 1 mM H_2Q solution. The i_d vs. $t^{-1/2}$ curve for the oxidation at the bare electrode (with a potential step from 0.0 to +0.4 V

(20) Greenland, D. J. *J. Colloid Sci.* **1963**, *18*, 647.
(21) Peerce, P.; Bard, A. J. *J. Electroanal. Chem.* **1980**, *112*, 97.
(22) Leddy, J.; Bard, A. J.; *J. Electroanal. Chem.* **1983**, *153*, 223.
(23) Ikeda, T.; Schmehl, R.; Denisevich, P.; William, K.; Murray, R. W. *J. Am. Chem. Soc.* **1982**, *104*, 2683.
(24) Gueshi, T.; Tokuda, K.; Matsuda, H. *J. Electroanal. Chem.* **1978**, *89*, 249.
(25) Gueshi, T.; Tokuda, K.; Matsuda, H. *J. Electroanal. Chem.* **1979**, *101*, 29.
(26) Gough, D. A.; Leypoldt, J. K. *Anal. Chem.* **1979**, *51*, 439.
(27) Gough, D. A.; Leypoldt, J. K. *Anal. Chem.* **1980**, *52*, 1126.
(28) Gough, D. A.; Leypoldt, J. K. *J. Electrochem. Soc.* **1980**, *127*, 1278.
(29) Itaya, K.; Bard, A. J., submitted for publication.

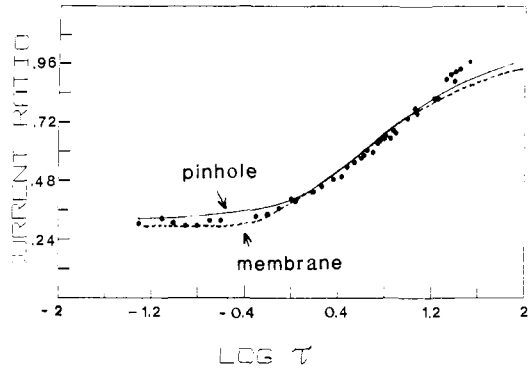

Figure 4. Chronoamperometric measurements on 1 mM H_2Q in pH 7 buffer for potential step from 0 to 0.4 V vs. SSCE. Variation of the current ratio as a function of log τ; theoretical curve for the pinhole (—) and the membrane (---) model.

vs. SSCE) was linear with a zero intercept, as predicted for an uncomplicated electrode reaction,[30] and yielded a solution diffusion coefficient (D_s) for H_2Q of 1.2×10^{-5} cm^2 s^{-1} compared to a D_s = 1.7×10^{-5} cm^2 s^{-1} from RDE experiments. With films of dry thicknesses (d) of 0.5 to 3 μm, the observed currents at a given t were smaller than at the bare electrode; a plot of the current ratio, $i(t)/i_d(t)$, vs. t is given in Figure 4. As predicted by both the pinhole and membrane models, the ratio is constant and less than unity at short times and then rises over an intermediate time range toward unity.

The chronoamperometric results fit both pinhole[21,24,25] and membrane[21] models. The calculated pinhole diameters, 31–79 μm, appear unreasonably large, many times the film thickness and of a size that should be readily observable. No pinholes were observed when clay films were examined under a microscope at 1500× magnification. However, negatively charged species such as $C_2O_4^{2-}$, $Mo(CN)_8^{4-}$, and I^-, which would be expected to be repelled by the clay, do penetrate clay films, suggesting the presence of channels between the clay particles.

On the other hand, the results also fit the membrane model. The diffusion coefficients for H_2Q (D_m = 1.0×10^{-7} cm^2 s^{-1}), determined by fitting the chronoamperometric data to the membrane model, are consistent with the D_m values obtained from chronoamperometric plots at very short times (D_m = 1.2×10^{-7} cm^2 s^{-1}) and steady-state measurements using rotating disk voltammetry (D_m = 1.2×10^{-7} cm^2 s^{-1}). For these calculations, the film thickness used was that of a dry clay film, K = 5, and D_s = 1.7×10^{-5} cm^2 s^{-1}.

Nonlinear Levich plots and linear Koutecky–Levich plots with a nonzero intercept and slope equal to that at a bare electrode were also obtained for the diffusion of H_2Q through clay films in rotating disk electrode experiments. The intercepts for the Koutecky–Levich plots were inversely proportional to the bulk solution concentration, C_0*, and directly proportional to film thickness, d. We have recently found tha clay layers that have been pillared by various treatments (e.g., with hydroxyaluminum) show much smaller penetration of anionic species.[29]

Electrochemistry of Ions Incorporated into Clay Films. Many positively charged electroactive species are held very strongly by smectite clays as exchangeable cations. Here we report the electrochemistry of several clay-bound species.

While our earlier communication[1] implied that ions incorporated into montmorillonite layers in the absence of PVA showed greatly reduced electroactivity, we have found that some clay films alone form coatings which show voltammetric responses of incorporated ions. The extent of electroactivity of these films strongly depends upon the length of time the film is soaked in the solution of electroactive ion, its concentration, the mode of preparation of the clay, the film thickness, and the identity of the incorporated ion. In the presence of PVA more uniform films are formed and

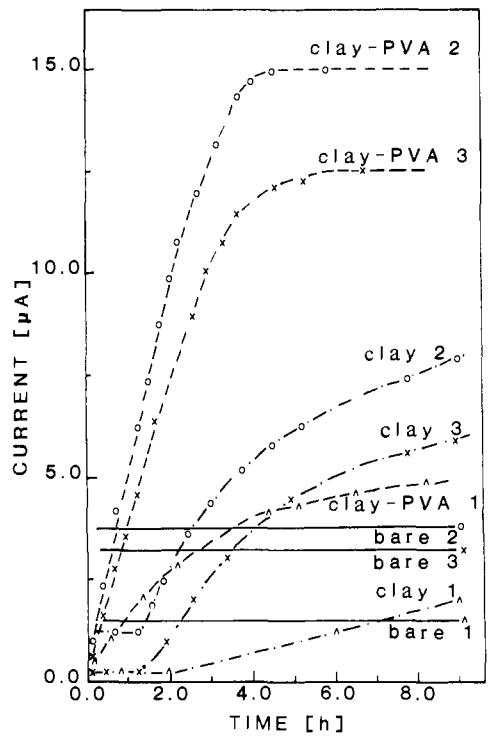

Figure 5. Anodic peak current vs. immersion time at bare SnO_2, clay (STx-1)SnO_2, and clay (STx-1)/PVA/SnO_2 electrodes soaked in 0.1 mM (1) $Fe(bpy)_3^{2+}$, (2) $Ru(bpy)_3^{2+}$, and (3) $Os(bpy)_3^{2+}$ solutions containing 0.05 M Na_2SO_4 (pH 7). Electrode area 0.4 cm^2 ($d \sim 1$ μm).

the rate of appearance of electrochemical response upon soaking the film in a solution of electroactive ion is enhanced. The electrochemical behavior at a bare, a clay, and a clay–PVA electrode was also studied when these were soaked (with continuous cycling) in solutions containing 0.1 mM $Fe(bpy)_3^{2+}$, $Ru(bpy)_3^{2+}$, or $Os(bpy)_3^{2+}$. All of these show well-defined cyclic voltammograms, and the anodic peak current (i_{pa}) can be used to monitor the incorporation with time (Figure 5). With PVA-containing clay films, the maximum peak current, i_{pa}, was observed after 4–5 h of soaking in a 0.1 mM $Fe(bpy)_3^{2+}$, $Ru(bpy)_3^{2+}$, or $Os(bpy)_3^{2+}$ solution. This current was at least three times larger than the peak current at a bare electrode in the same solution containing the electroactive species. At a clay-modified electrode (without PVA), and up to soaking times of 0.5 h, the electrochemical response was very small compared to the bare electrode. After this initial soaking time, there was a continuous increase in the measured peak current. The rate of increase of i_{pa} as a function of soaking time varied as follows: $Ru(bpy)_3^{2+}$ > $Os(bpy)_3^{2+}$ > $Fe(bpy)_3^{2+}$ (Figure 5). Note that the above results were obtained in a solution containing the electroactive species. Smaller currents were observed when the clay-modified electrode was transferred to a solution containing only the supporting electrolyte solution. These results demonstrate binding of the cations in the clay film, either on the surface of the particles, intercalated between the clay layers, or through intersalation of the metal complex[31] salt, leading to binding of metal complex beyond the cation exchange capacity of the clay.

For thicker films (>0.2 μm), the voltammograms exhibited diffusional behavior. However, direct dependence of the $Ru(bpy)_3^{2+}$ anodic peak current i_{pa} on the sweep rate, v, and wave shapes characteristic of "thin film behavior" have been observed with relatively thin (30–200 nm) clay films, e.g., (SWy-1)–Pt/PVA–$Ru(bpy)_3^{2+}$–GCE at small v (Figure 6). Even when such thin film behavior was found, the difference between anodic and cathodic peak potentials, ΔE_p, for the $Ru(bpy)_3^{2+/3+}$ reaction was 100 to 150 mV. The oxidation peak potential (E_{pa}) shifted to more

(30) Bard, A. J.; Faulkner, L. R. "Electrochemical Methods"; Wiley and Sons: New York, 1980; p 143.

(31) Traynor, F. S. E.; Mortland, M. M.; Pinnavaia, T. J. *Clay Clay Miner.* **1978**, *26*, 318.

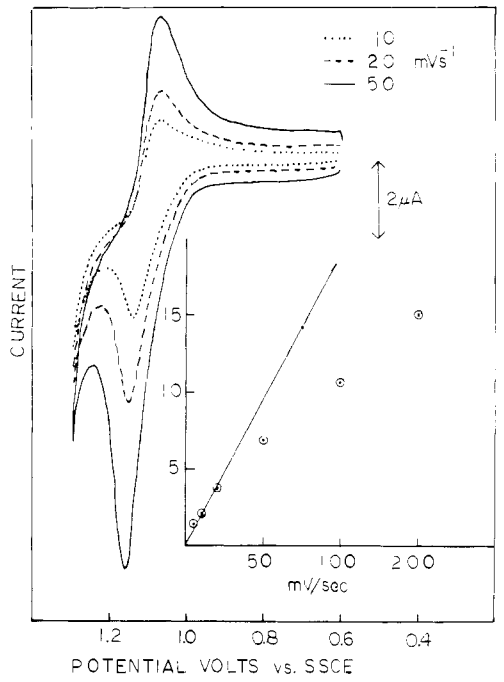

Figure 6. Cyclic voltammograms at a clay (SWy-1)/Pt/PVA/Ru(bpy)$_3^{2+}$/GCE in 0.05 M Na_2SO_4 (pH 7) as a function of sweep rate: 10 mV s^{-1} (···), 20 mV s^{-1} (---), and 50 mV s^{-1} (—). Inset, i_{pa} dependence on v.

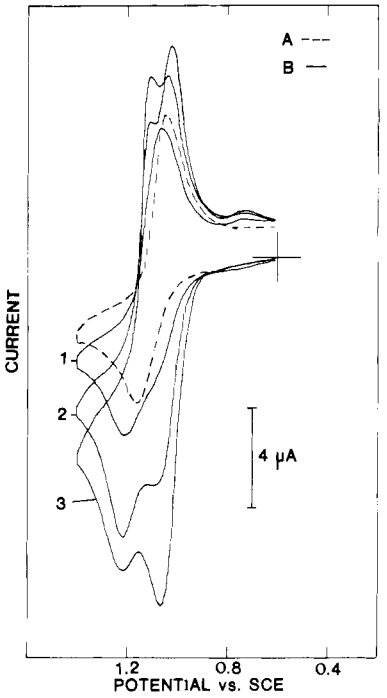

Figure 7. Cyclic voltammograms comparing the electrochemical response at (A) a clay (STx-1)/Ru(bpy)$_3^{2+}$/SnO_2 electrode in 0.1 M Na_2SO_4 (---) and (B) in 1 mM Ru(bpy)$_3^{2+}$ (—) at a sweep rat of 50 mV s^{-1}, A = 0.5 cm^2. The numbers 1, 2, and 3 refer to first, second, and third scan after the electrode was transferred into Ru(bpy)$_3^{2+}$ solution.

positive values with increasing sweep rate, indicating slow electron transfer kinetics or resistance effects. The E_{pa} value for Ru(bpy)$_3^{2+}$ incorporated into the clay film was shifted to more positive values by ca. 100 mV relative to that of the solution species. When the clay-modified electrode containing Ru(bpy)$_3^{2+}$ was immersed in a 1 mM Ru(bpy)$_3^{2+}$ solution, and voltammetric scans taken immediately, an oxidation peak ca. 100 mV negative of that for bound Ru(bpy)$_3^{2+}$ in 0.1 M Na_2SO_4 alone appeared, and the peak current grew with time caused by extraction of more Ru(bpy)$_3^{2+}$ into the film (Figure 7). The E_{pa} value of this more negative peak was the same as that of Ru(bpy)$_3^{2+}$ in solution; its peak current was usually almost the same or slightly smaller than that obtained at a bare SnO_2 electrode. With time, these two oxidation peaks merged and appeared as a single peak. The peak current of this single peak was smaller than the sum of the peak currents for Ru(bpy)$_3^{2+}$ in solution and Ru(bpy)$_3^{2+}$ in the film (as observed in 0.1 M Na_2SO_4), probably because diffusion of the solution species through the film is retarded. A shift in the redox (formal) potentials was also observed by Tsou and Anson[32] upon incorporation of cationic complexes in perfluoropolycarboxylate and polysulfonate films. For example, they reported that steady-stae cyclic voltammograms for a 1 mM solution of Ru(NH$_3$)$_6^{3+}$ at a graphite electrode coated with a perfluoropolycarboxylate gave two clearly separated oxidation peaks. The peak which was present only in solutions containing Ru(NH$_3$)$_6^{3+/2+}$ was attributed to direct oxidation–reduction of the complex at the electrode surface, diffusing through the film.

Characteristic thin film (as opposed to diffusive) behavior was observed at spin-coated clay electrodes (thickness, d = 0.03–0.2 μm) in 0.01 M Na_2SO_4 with incorporated Os(bpy)$_3^{2+}$ and Fe(bpy)$_3^{2+}$. The first scan in the positive direction and the following scan, for a 0.06 μm coated clay (SWy-1)–Os(bpy)$_3^{2+}$–SnO_2 electrode in 0.01 M Na_2SO_4, is shown in Figure 8A. The change in the cyclic voltammetric behavior as a function of sweep rate in 0.01 M Na_2SO_4, is shown in Figure 8B for a 0.03 μm STx-1–clay film soaked in Os(bpy)$_3^{2+}$ for 6 min. The anodic peak current, i_{pa}, is directly proportional to v, up to 20 mV s^{-1}; at sweep rates ≥60 mV s^{-1}, i_{pa} is proportional to $v^{1/2}$. The peak current in the diffusion-controlled region in Figure 8B was used to calculate a diffusion coefficient for Os(bpy)$_3^{2+}$ incorporated in clay, yielding D_m = 1.2 × 10^{-12} cm^2 s^{-1}. The number of moles of electroactive species was obtained by integrating the area under the oxidation peak at 5 mV s^{-1}, for Os(bpy)$_3^{2+}$ (2.6 × 10^{-10} mol, corresponding to a 12% loaded film assuming a density of 2 g/cm^3 and cec of 1 mequiv/g of clay). The dry thickness of the film was 0.03 μm, and the electrode had an area of 0.7 cm^2. Thus, the effective concentration of the Os(bpy)$_3^{2+}$ in the film was about 0.1 M. The Os(bpy)$_3^{2+}$ incorporated into these clay films was not leached out after soaking in 0.1 M Na_2SO_4 for several hours. There was a negative shift of 100 mV in the potential for oxidation and a decrease (up to ca. 50%) in i_{pa} after the first positive scan. However, after this initial break in, the peak currents did not change for at least 1 h even under repetitive scanning at v = 2 mV s^{-1}. When the Os(bpy)$_3^{2+}$ incorporated in a clay film was left in electrolyte solution for ca. 12 h, the electrochemical signal decreased to half of its original value. When thicker films were used, for example, ca. 0.2 μm, there was a constant decrease in the observed peak currents until a steady-state current was reached (Figure 9A). The electrochemical behavior of Ru(bpy)$_3^{2+}$ incorporated into clay was quite different from that of Os(bpy)$_3^{2+}$ bound to clay. Cyclic voltammograms in Figure 9A show typical electrochemical responses at a clay (SWy-1)–Os(bpy)$_3^{2+}$–SnO_2 electrode in 0.1 M Na_2SO_4. The peak currents for the Os(bpy)$_3^{2+/3+}$ couple constantly decrease, suggesting a loss of incorporated electroactive species with time. There was also a decrease in i_{pa} for Ru(bpy)$_3^{2+}$ (Figure 9B). Electrolysis of Os(bpy)$_3^{2+}$ incorporated into thin clay films was complete in ca. 0.5 h, whereas it took over 2 h to oxidize completely the Ru(bpy)$_3^{2+}$ bound to similar clay films. The ratio of the number of coulombs passed during the reduction of the electrochemically generated Ru(bpy)$_3^{3+}$ to the number of coulombs passed during the oxidation of Ru(bpy)$_3^{2+}$ was 0.2. On the basis of these coulometric results and cyclic voltammetric behavior, which will be discussed further in a later section, we believe that there is a chemical reaction between the electrogenerated Ru(bpy)$_3^{3+}$ and some clay species to regenerate Ru(bpy)$_3^{2+}$. CV behavior of Fe(bpy)$_3^{2+}$ incorporated in thin clay films was similar to that of Os(bpy)$_3^{2+}$ ($i_{pa} \propto v$ up to 10 mV s^{-1} and D = 1.2 × 10^{-12} cm^2 s^{-1} from CV's at different sweep rates). The ΔE_p was 15 mV and the potential full width

(32) Tsou, Y.-M.; Anson, F. C. *J. Electrochem. Soc.* **1984**, *131*, 595.

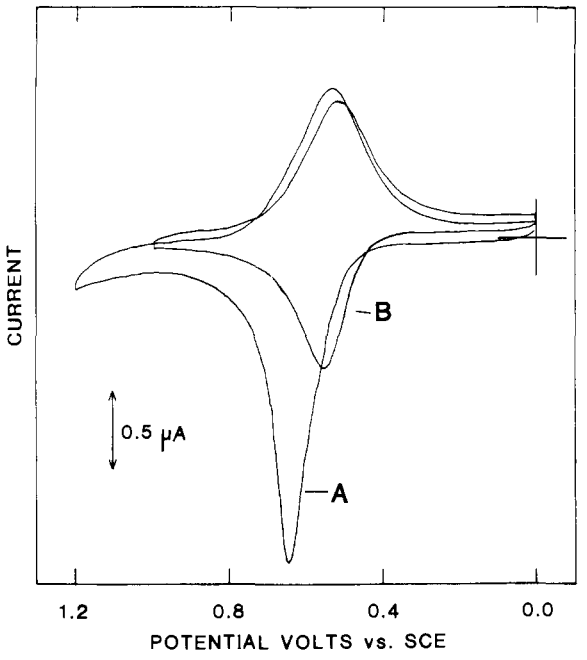

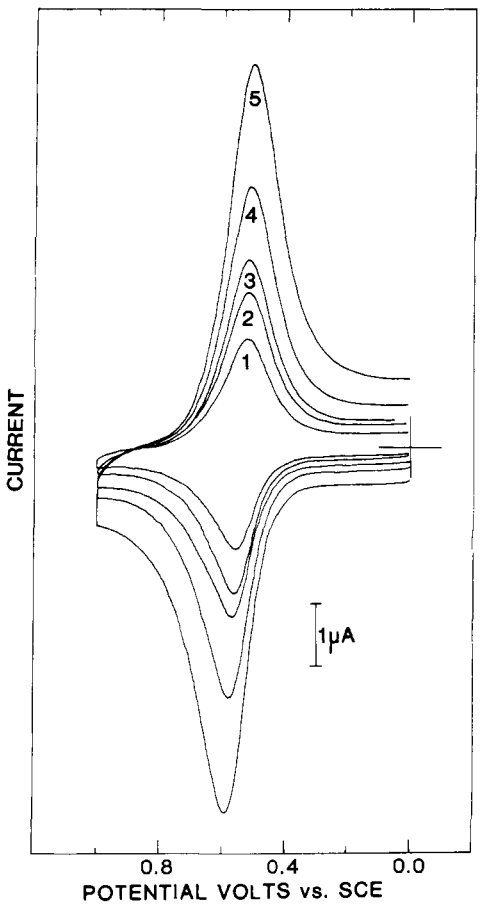

Figure 8. Cyclic voltammograms at a spin-coated clay (SWy-1)–Os-$(bpy)_3^{2+}$–SnO_2 electrode in 0.1 M Na_2SO_4: (A) first scan, (B) second and the following scans, v = 2, mV s^{-1}, film thickness 60 nm, A = 0.7 cm^2. Cyclic voltammograms at a spin coated clay (SWy-1)–Os-$(bpy)_3^{2+}$–SnO_2 electrode, ~30 nm thick, A = 0.7 cm^2, as a function of sweep rate: (1) 10, (2) 15, (3) 20, (4) 30, (5) 50 V s^{-1}.

at half maximum, E_{fwhm}, was 110 mV, at v = 1 mV s^{-1}. Cyclic voltammograms with a 0.05 μm thick clay (STx-1)–Fe-$(bpy)_3^{2+}$–SnO_2 electrode in 0.01 M Na_2SO_4 are shown in Figure 10 at different sweep rates. Note that between v = 2.5 and 7.5 mV s^{-1}, the values of ΔE_p do not change, indicating that the rate of charge transfer is fast at these sweep rates. When the films

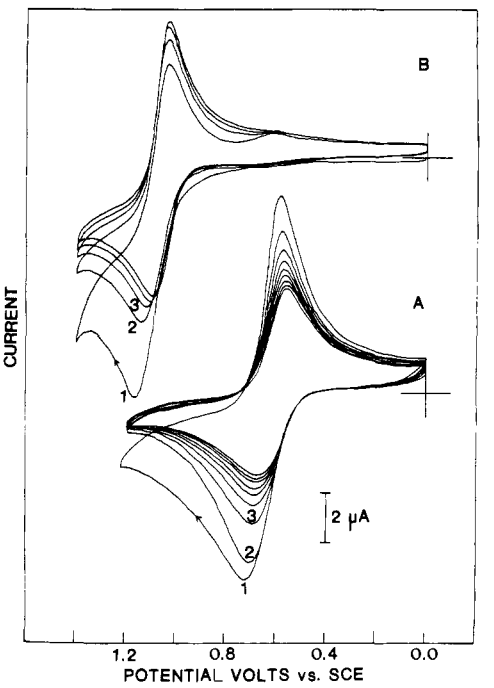

Figure 9. Repetitive voltammograms of (A) $Os(bpy)_3^{2+}$ and (B) Ru-$(bpy)_3^{2+}$ incorporated into clay (SWy-1)/SnO_2 electrodes in 0.1 M Na_2SO_4 at a sweep rate of 10 mV s^{-1}, A = 0.5 cm^2, d = 0.2 μm.

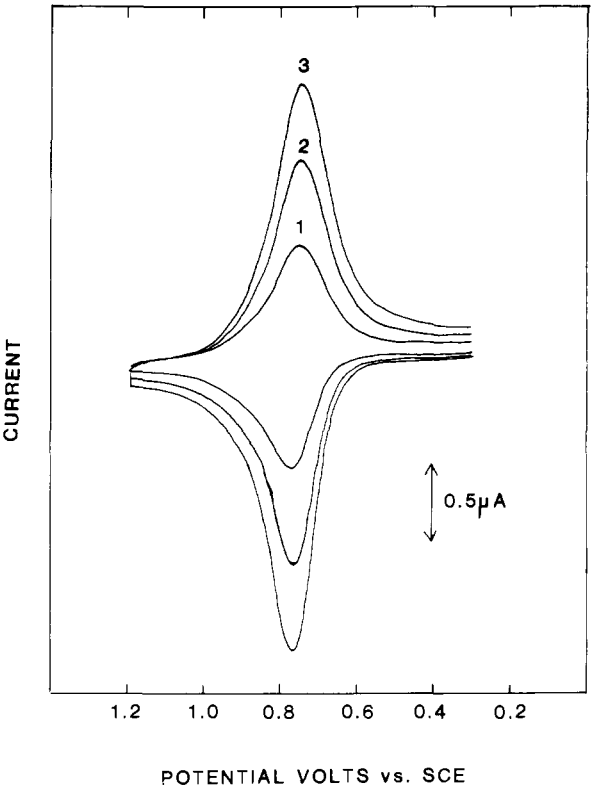

Figure 10. Cyclic voltammograms at a spin coated clay (STx-1)/Fe-$(bpy)_3^{2+}$/SnO_2 electrode in 0.01 M Na_2SO_4 at (1) 2.5, (2) 5, and (3) 7.5 mV s^{-1}, A = 0.7 cm^2, d = 50 nm.

are made thicker, even at very slow sweep rates (e.g., v = 2 mV s^{-1}) diffusional tailing occurs and $i_p \propto v^{1/2}$.

When the clay electrodes were soaked for an extended period of time in $Ru(bpy)_3^{2+}$ containing solution, the cyclic voltammetric behavior in the inert electrolyte solution also suggested the presence of a chemical reaction. During the first CV cycle a large oxidation peak was observed with almost no reduction peak on the reverse sweep (Figure 11). The ratio of the peak currents i_{pc} to i_{pa} varied as a function of sweep rate (i.e., i_{pc}/i_{pa} was small at slow sweep

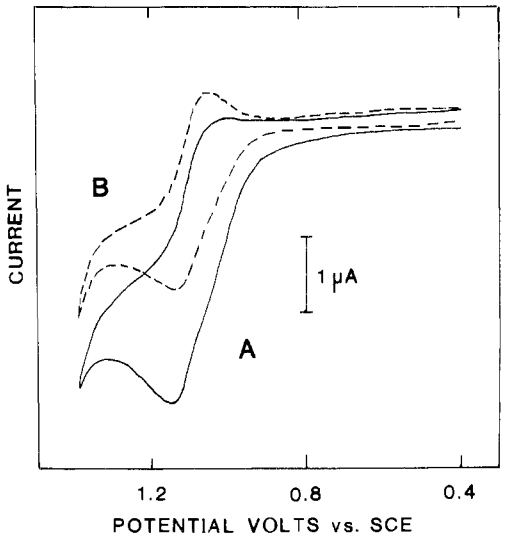

Figure 11. Cyclic voltammograms demonstrating the behavior of a clay (SWy-1)/$Ru(bpy)_3^{2+}$/SnO_2 after prolonged soaking in 1 mM $Ru(bpy)_3^{2+}$: (A) first sweep, (B) 10th sweep. At a sweep rate of 2 mV s^{-1} in 0.1 M Na_2SO_4.

rates and closer to one at higher sweep rates). The i_{pa} decreased during repetitive scans, suggesting that the species involved in the chemical reaction with $Ru(bpy)3^{3+}$ was consumed (Figure 11). The nature of this chemical reaction was the same as that observed at a clay or clay–PVA modifed electrode in a solution containing 0.1 mM $Ru(bpy)_3^{2+}$ or $Fe(bpy)_3^{2+}$ during the first two cyclic voltammetric scans. The reaction was less pronounced with $Fe(bpy)_3^{2+}$ than with $Ru(bpy)_3^{2+}$, as indicated by the relative ratios of i_{pc}/i_{pa}. These results can be interpreted as electrochemically generated $Ru(bpy)_3^{3+}$ or $Fe(bpy)_3^{3+}$ reacting with a clay species to form $Ru(bpy)_3^{2+}$ or $Fe(bpy)_3^{2+}$. When a solution of $Ru(bpy)_3^{3+}$, which was obtained by chemical oxidation of $Ru(bpy)_3^{2+}$ with PbO_2 in acidic solution, was mixed with colloidal clay, an immediate reduction of $Ru(bpy)_3^{3+}$ to $Ru(bpy)_3^{2+}$ took place as indicated by the production of the orange color of $Ru(bpy)_3^{2+}$. Similarly, when a colloidal clay solution was mixed with $Os(bpy)_3^{3+}$ solution, $Os(bpy)_3^{2+}$ formed. However, the chemical nature of this reductant inside the clay is unknown at this point. Clays have been reported to react with a number of compounds in acid–base and/or redox reactions. Recently, Soma et al.[33] reported oxidation of benzene and *p*-phenylene to poly-*p*-phenylene cations in the presence of clays.

We also investigated the CV behavior as a function of the concentration of $Ru(bpy)_3^{2+}$ in a clay (SWy-1)/Pt/PVA film. The cathodic peak current, i_{pc}, was directly proportional to the film absorbance (where absorbance at 468 nm is proportional to concentration) which demonstrates that i_{pc} varies linearly with $Ru(bpy)_3^{2+}$ concentration. This suggests that D_{app} does not change with film concentration and that the fraction of clay-contained species that is electroactive (f) is constant at all concentration levels. This fraction, f, depends upon film thickness and method of preparation of the clay layer. For a ca. 1 μm thick film which contained clay (STx-1)–PVA–$Ru(bpy)_3^{2+}$ the value of f was estimated as follows. For a film absorbance of 1.110 the surface concentration (Γ_{total}) of $Ru(bpy)_3^{2+}$ was 5.3×10^{-8} mol/cm^2 (ϵ_{468} = 21 000 M^{-1} cm^{-1}). For the same film where $Q = 8.1 \times 10^{-4}$ C cm^{-2} $Ru(bpy)_3^{2+}$ was first oxidized and then reduced (Q reported here corresponds to the number of coulombs passed during reduction). Hence, $\Gamma_{electroactive} = 8.4 \times 10^{-9}$ mol/cm^2, and f is ca. 0.18, i.e., only 18% of the $Ru(bpy)_3^{2+}$ in this film was electroactive. We also estimated the maximum loading level achieved in a typical film. A SnO_2 electrode, area ca. 1 cm^2, was coated with 50 μL of a clay–PVA mixture, the clay concentration being 6.5 g/L. For a cec value of 76.4 mequiv/100 g, the number of monocationic exchange sites in the film is 2.5×10^{-7} equiv cm^{-2}. Hence, the

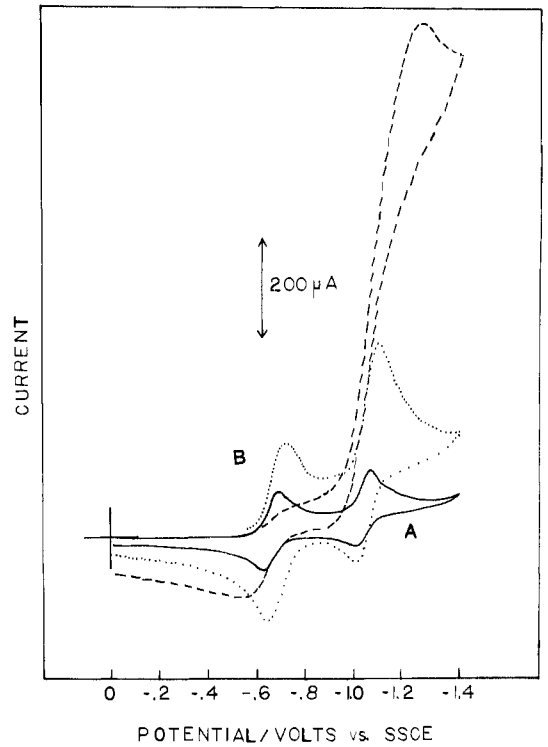

Figure 12. Cyclic voltammograms of a 2 mM PVS solution in pH 7 phosphate buffer at (A) bare SnO_2 (—), (B) clay (SWy-1)/SnO_2, and (C) clay (SWy-1)/Pt/PVA–SnO_2 electrode at a sweep rate of 50 mV s^{-1}.

maximum concentration of $Ru(bpy)_3^{2+}$ (dication) that could be held at anionic sites is 1.25×10^{-7} mol cm^{-2}. The maximum surface concentration calculated from our absorbance measurements was ca. 4.7×10^{-8} mol cm^{-2}, i.e., ca. 43% of the cec sites are occupied. The films used for these measurements were dried at low heat and soaked in 1 mM $Ru(bpy)_3^{2+}$ solution until a constant absorbance value was obtained. Before making absorbance measurements, the filmed SnO_2 electrodes were rinsed with distilled H_2O and placed in a vial containing just H_2O for several minutes to wash out any $Ru(bpy)_3^{2+}$ which did not bind to the clay.

Details of the mechanisms of charge transport within these films remain to be elucidated. The small D values calculated for $Os(bpy)_3^{2+}$ and $Fe(bpy)_3^{2+}$ bound to clay films ($D = 1.2 \times 10^{-12}$ cm^2 s^{-1}) demonstrate slow physical movement and charge hopping. A recent literature report suggested a D value between 10^{-10} and 10^{-8} cm^2 s^{-1} for $Ru(bpy)_3^{2+}$ in extensively hydrated colloidal clay particles.[34] D may be smaller in ordered clay films, since interlayer migration (migration from one sheet to another) is likely to be very inefficient (e.g., because it is difficult for the ions to overcome the electrostatic barrier at the layer boundaries). Charge transfer in polyelectrolyte films into which ionic redox groups have been incorporated by ion-exchange takes place by electron hopping or molecular diffusion.[35-38] Similar processes probably occur in the clay films.

Electrochemistry of Propyl Viologen Sulfonate (PVS). To extend our studies of the diffusion of uncharged solution species through clay films, the electrochemistry of the uncharged propyl viologen sulfonate (PVS) was investigated at clay-modified

(33) Soma, Y.; Soma, M.; Honada, J. *J. Phys. Chem.* **1984**, *88*, 3034.

(34) Mahti, A.; Keravis, D.; Levitz, P.; Van Damme, H. *J. Chem. Soc., Faraday Trans. 1* **1984**, *280*, 67.

(35) Murray, R. W. "Electroanalytical Chemistry"; Bard, A. J., Ed., Marcel Dekker: New York, 1984; p 334.

(36) Buttry, D. A.; Anson, F. C. *J. Electroanal. Chem.* **1981**, *130*, 333.

(37) White, H. S.; Leddy, J.; Bard, A. J. *J. Am. Chem. Soc.* **1982**, *104*, 4811.

(38) On the basis of our recent ESR studies (Gaudiello, J.; Ghosh, P. K.; Bard, A. J. *J. Am. Chem. Soc.* **1985**, *107*, 3027), charge transport by physical diffusion of ions has also been inferred for MV^{2+} in Nafion films.

electrodes. In contrast to the behavior observed in H_2Q solutions, the peak currents in the cyclic voltammogram were larger (2–4 times) at the clay-modified electrode (without Pt/PVA) (Figure 12B) than at the bare electrode (Figure 12A). Clearly PVS is extracted into the film with $K > 1$. Other than the increase in peak currents, the voltammetric profiles were similar at the coated and uncoated electrodes. The cyclic voltammogram was very different, however, when clay films were cast from a clay–Pt/PVA mixture. Here, the reversible voltammograms were replaced by a single cathodic wave (Figure 12C). The absence of an anodic wave suggests oxidation of the electrogenerated reduced viologen in a chemical step. Clay films cast from clay–PVA mixtures not containing Pt do not exhibit such behavior; instead, reversible voltammograms are obtained as in pure clay films. Hence, it is dispersed platinum in the clay films which promotes the reduction of a solution species with regeneration of PVS (a catalytic or EC′ mechanism).[39] The above results are analogous to those observed at clay–RuO_2/PVA films, where RuO_2 promotes the oxidation of water in the presence of electrochemically produced $Ru^{III}(bpy)_2[bpy(CO_2)_2]^+$ with regeneration of the Ru^{II} complex.[2] For the clay–PVS–Pt/PVA system the voltammograms exhibit a marked pH dependence, with increased peak currents and positive shifts in the peak potential observed at lower pH values. We have not yet carried out extensive bulk coulometry to identify the product(s) of the reaction. However, the presence of H_2 has been detected in samples collected upon reduction of PVS at clay–Pt/PVA modified electrodes. We tentatively assign the catalytic step to Pt-mediated proton reduction and concomitant regeneration of PVS. Note that hydrogen formation has previously been observed in aqueous suspensions of colloidal Pt containing the viologen cation radical.[40,41]

Conclusions

We can propose a tentative model for the structure and electrochemical processes within the clay films based on these experiments. The relative electroactivity of species incorporated in the films depends upon the degree of swelling and the spacing between particles and layers. The ESR and XRD measurements suggest that the films cast from clay alone are oriented (Figure 2A). The rate of incorporation of electroactive cationic species and their effective mobilities within the film depend upon the pretreatment and time such films are soaked in the aqueous solutions. The role of the PVA and Pt/PVA is then to assist in the swelling of the films to increase the mobility of the incorporated ions. The effect of PVA on clays has been discussed previously.[20] The PVA residues on the surface of the clay sheets and decreases the Coulombic forces between the fixed negative sites on the clay and the cationic species (Figure 2C). Thus, the PVA increases cation mobility by expanding the clay lattice, promoting a more random and less packed distribution of the particles (as shown by the ESR and XRD results), and decreasing the interaction of cations with the particle surfaces. This interaction must be an important factor in the physical mobility of incorporated species, since uncharged forms, e.g., PVS and $Ru(bpy)_2[bpy\text{-}(CO_2)_2]$, show enhanced activity compared to the corresponding cationic forms, MV^{2+} and $Ru(bpy)_3^{2+}$. Note that there is no apparent incorporation of ions, observed electrochemically, when PVA or Pt/PVA (without clay) are cast on electrode surfaces, so that one cannot consider these to be PVA polymer-modified electrodes with the clay merely extending the available surface area. There are probably several sites possible for the incorporated ions, i.e., adsorbed on surfaces and edges and intercalated between layers. Such "strongly interacting" species are only slowly leached from the clay films. The effective diffusion coefficients of these species (representing physical movement, and perhaps, charge hopping) is $\sim 10^{-12}$ cm^2/s, which is smaller than in most polymer films. Uncharged and anionic species are not strongly held by the film, but these can penetrate the film to the substrate surface, probably via small channels, in a membrane-like process. While electrocatalysis has been demonstrated with these electrodes, e.g., with PVS/Pt and with $Ru(bpy)_2[bpy(CO_2)_2]/RuO_2$,[2] electrochemical exploitation of the unique intercalation and steric environment[7] of the clay film awaits further studies.

Acknowledgment. We appreciate the support of this research by the National Science Foundation (CHE8402135) and a grant from IBM. Support by the Schweizerische National Fonds zur Foerderung der Wissenschalficher Forschung to J.F.E. is also gratefully acknowledged.

Registry No. 1, 14691-88-4; PVA, 9002-89-5; PVS, 77951-49-6; H_2Q, 123-31-9; SWy-1, 1318-93-0; $Os(bpy)_3^{2+}$, 23648-06-8; $Ru(bpy)_3^{2+}$, 15158-62-0; $Fe(bpy)_3^{2+}$, 15025-74-8; Na_2SO_4, 7757-82-6; SnO_2, 18282-10-5; Pt, 7440-06-4; C, 7440-44-0; H_2, 1333-74-0.

(39) Reference 30, pp 455–460.
(40) Moradpour, A.; Amouyal, E.; Keller, P.; Kagen, H. *Nouv. J. Chim.* **1978**, *2*, 547.
(41) Kiwi, J.; Gratzel, M. *J. Am. Chem. Soc.* **1979**, *101*, 7214.

Cesium Desorption Ionization Studies of β-Cyclodextrin by Fourier Transform Mass Spectrometry

M. E. Castro, L. M. Mallis, and D. H. Russell*

Contribution from the Department of Chemistry, Texas A&M University, College Station, Texas 77843. *Received August 22, 1984*

Abstract: The mass spectra of β-cyclodextrin obtained by Cs^+ desorption ionization–Fourier transform mass spectrometry are reported. The results from this study illustrate the effects of the Cs^+ ion beam density on the yield of molecule ions of the type $[M+H]^+$ vs. organoalkali ions of the type $[M+Na]^+$, $[M+Na(NaX)_n]^+$, and $[M+xNa-(x-1)H]^+$ and fragment ions. It is shown that high beam densities favor formation of the organoalkali metal ions, and that abundant $[M+H]^+$ molecule ions are formed only at low beam densities. A general mechanism for formation of the organoalkali metal ions is presented, and this mechanism is supported by studies using fast-atom bombardment (FAB) ionization in conjunction with tandem mass spectrometry (TMS). The results from FAB–TMS studies suggest that ions of the types $[M+Na(NaX)_n]^+$ and $[M+xNa+(NaX)_{n-x}-(x-1)H]^+$ dissociate to produce the organoalkali metal ions, e.g., $[M+Na]^+$ and $[M+xNa-(x-1)H]^+$. Based on these results it is suggested that ions of the types $[M+Na]^+$ and $[M+xNa-(x-1)H]^+$ produced directly by desorption ionization are formed by dissociation of $[M+Na(NaX)_n]^+$ and $[M+xNa+(NaX)_{n-x}-(x-1)H]^+$ ions.

Desorption ionization (DI) has evolved into a routine chemical analysis method for nonvolatile, thermally labile organic molecules.[1] Rapid growth has occurred in this area since the introduction of fast-atom bombardment (FAB) or liquid secondary-ion

0002-7863/85/1507-5652$01.50/0